RSC Advances

ROYAL SOCIETY OF CHEMISTRY

www.rsc.org/advances

Structural, spectroscopic and magnetic properties of a novel copper(II) L-tyrosinato complex

Agnieszka Wojciechowska [a,*], Anna Gągor [b], Julia Jezierska [c], Marek Duczmal [a]

[a] Faculty of Chemistry, Wrocław University of Technology, Wybrzeże Wyspiańskiego 27, 50-370 Wrocław, Poland

[b] Institute of Low Temperature and Structure Research Polish Academy of Sciences, Okólna 2, 50-422 Wrocław, Poland

[c] Faculty of Chemistry, University of Wrocław, F. Joliot-Curie 14, 50-383 Wrocław

AUTHOR EMAIL ADDRESS agnieszka.wojciechowska@pwr.edu.pl

Corresponding Author. Agnieszka Wojciechowska, Faculty of Chemistry, Wrocław University of Technology, Wybrzeże Wyspiańskiego 27, 50-370 Wrocław, Poland Phone: +48 713203666; Fax: +48 71 320 43 60.

ABSTRACT : The complex $[Cu(L\text{-}Tyr)_2(H_2O)]\cdot H_2O$ (**1**) (where L-Tyr = L-tyrosine) was obtained as crystals and characterized by X-ray, spectroscopic (FT-IR, FT-Raman, NIR-vis-UV, and EPR) and magnetic methods. The monomeric complex crystallized in the monoclinic $P2_1$ symmetry with a = 11.967 (1) Å, b = 5.9986 (4) Å, c = 14.936 (1) Å. The amino N and carboxylate O atoms of chelating L-tyrosinate anions together with O atom of water molecules create a slightly distorted square pyramidal environment around Cu(II) ions (τ = 0.11). The distant of about 5.998(1)Å $[Cu(L\text{-}Tyr)_2H_2O]$ units are involved in a polymeric chain based on N(1)—H···O(4)^{vi} and N(2)—H···O(5)^{vi} hydrogen bonds. The *d-d* band found in polycrystalline-reflectance spectrum at 15700 cm^{-1} is composed of three $^2B_1(d_{x2-y2}) \rightarrow {}^2A_1$ (d_{z2}), $^2B_1 \rightarrow {}^2B_2(d_{xy})$ and $^2B_1 \rightarrow {}^2E$ ($d_{xz} \approx d_{yz}$) transitions with energies 14880, 15800 and 19950 cm^{-1}, respectively. In DMSO solution the complex preserves its square pyramidal geometry as evidenced by intensive band at *ca.* 16400 cm^{-1}. The EPR spectral parameters for powder (g_{II} = 2.236 and $g_\perp$ = 2.063) and DMSO frozen solution ($g_\parallel$ = 2.250, $g_\perp$= 2.055,and $A_\parallel$ = 180 G) correspond to an axial symmetry of Cu(II) coordination geometry with d_{x2-y2} orbital as a ground state of the unpaired electron. Furthermore, the frozen solution spectrum revealed the signals corresponding to S=1 spin states of Cu(II) ions coupled by dipole-dipole interactions with distinctly resolved hyperfine splitting due to two copper nuclei ($|D|$ = 0.0468 cm^{-1}, $g_\parallel$ = 2.238, $g_\perp$ = 2.06 and $A_\parallel$ = 85 G). The variable-temperature magnetic susceptibility measurements revealed the existence of a weak ferromagnetic interaction between neighboring copper(II) ions through the N—H···O hydrogen bonds.

Keywords *copper(II) complex; L-tyrosine; X-Ray structure; FT-IR; FT-Raman; NIR-Vis-UV electronic spectroscopy; EPR spectroscopy; magnetic susceptibility;*

Introduction

2-amino-3-(4-hydroxyphenyl)propionic acid, referred to as L-tyrosine (L-Tyr), is a very important endogenic amino acid and a precursor of : thyroid hormones as triiodothyronine (T_3) and tyroxine (T_4) [1]; neurotransmitters as dopamine [2], noradrenaline [3], adrenaline [3]; alkaloid morphine [2] and mescaline [4] and, also, the natural pigment – melanin [5]. L-tyrosine, as well as other amino acids, forms coordination bonds with metal ions. These metal ions complexes are structural, spectroscopic, magnetic characterized [6-12] and tested against bacterial [13-14] or fungal [13-15] strains. However, their biological properties are relatively rarely evaluated.

First literature report of L-tyrosine interaction with copper(II) ion comes from 1968, when Van der Helm and co-workers published the results of a variation of the square-pyramidal copper(II) surrounded in a complex with glycyl-L-leucyl-L-tyrosine peptide [16]. The deprotonated amide nitrogen and carboxyl oxygen atoms of the L-tyrosyl residues together with glycyl nitrogen and oxygen atoms form a base of the square-pyramidal geometry around two copper(II) ions. Further refinement of this copper-peptide dimer crystal structure indicated the occurrence of two peptides and two copper atom in an asymmetric unit [17]. But, first crystal structure of copper(II) complex containing pure L-tyrosine was described in 1972 as a structure of *bis*-(L-tyrosinato)copper(II) complex [18]. Later, McAuliffe and co-workers studying the donor properties of this amino acid with Cu^{2+}, Ni^{2+}, Zn^{2+} ions obtained a powder of $[Cu(L\text{-}Tyr)_2H_2O]$ compound [19]. After that researchers drew attention to polymeric structure and expected magnetic properties of the *bis*-(L-tyrosinato)copper(II) complex [18], finally, they described it as a coordination polymer of formula $[Cu(L\text{-}Tyr)_2]_n$ [20-22]. In recent years, a narrow group of L-tyrosinato five-coordinated Cu(II) ion complexes has been extended by four new complexes consisting of aromatic diamine and water molecule located in vertices of a square-pyramid, characterized by crystal structure, spectroscopic and magnetic studies :

[Cu(L-Tyr)(2,2'-bpy)(H_2O)]Cl·3H_2O (2,2'-bpy = 2,2'-bipyridine) [23], [Cu(L-Tyr)(phen)(H_2O)]ClO_4·2.5H_2O [24], [Cu(L-Tyr)(phen)(H_2O)]ClO_4 [25] and [Cu(phen)(L-Tyr)(EA)]ClO_4 [26] (phen = 1, 10-phenanthroline, EA = ethylamine), [Cu(L-Tyr)(5,6-dmp)(H_2O)]ClO_4 (5,6-dmp = 5,6-dimethyl-1,10-phenanthroline) [27], [Cu(IP)(L-Tyr)(H_2O)]ClO_4·H_2O (IP = imidazol[4,5-*f*][1,10] phenanthroline) [28]. Especially, the [Cu(L-Tyr)(5,6-dmp)(H_2O)]ClO_4 complex is worth to mention, because of the studies of DNA cleavage and anticancer activity of this complex revealed its interaction with DNA of a calf thymic lymphocytes leading to the mitotic catastrophe and apoptotic cell death [27].

Further studies on the L-tyrosinato Cu(II) complexes are focused on investigating 3-iodo- and 3,5-diiodo-derivatives molecules. Both bioligands form crystalline complexes of square-pyramid geometry with water molecule in [Cu(2,2'-bpy)(L-Ityr)(H_2O)]·NO_3·CH_3OH·H_2O (L-Ityr = 3-iodo-L-tyrosine) [29], [Cu(hista)(L-I_2tyrO^-)(H_2O)]$_2$·2H_2O (L-I_2tyr = 3,5-diiodo-L-tyrosine) [29], [Cu(2,2'-bpy)(L-I_2tyrO^-)(H_2O)]·2H_2O [30], as well as nitrate(V) ion in [Cu(2,2'-bpy)(L-I_2tyrOH)(NO_3)]·CH_3OH [30]. The modification of phenolate ring leads to synthesizing the reduced Schiff base of benzaldehyde and L-tyrosine - Ph-TyrH ligand. This L-Tyr derivative interacts with copper(II) ion giving crystals of [Cu(Ph-Tyr)(L)(ClO_4)] [31] complex (Ph-Tyr = L-phenylalanine-L-tyrosine, L = phen or dppz = dipyrido[3,2-a:2',3'-c]phenazine).

L-tyrosine in combination with other amino acids forms various dipeptides. These compounds chelated Cu^{2+} ion and with bidentate organic N ligands and water molecule create five-coordinated copper(II) complexes *i.e* [Cu(L-Tyr-hist)] (L-Tyr-hist = L-tyrosyl-L-histidine) [32], [Cu(L-leucyl-L-tyrosine)(H_2O)] [33], [Cu(glycyl-L-tyrosine)(H_2O)$_2$]·2H_2O [34], [Cu(Gly-L-Tyr)(bzp)] [34] and [Cu(Gly-L-Tyr)(bzmp)] [19] (Gly-L-Tyr = glycyl-L-tyrosinate; bzp = N-benzyl-N-2-pyridylmethylamine; bzmp = N-benzyl-N-6-methyl-2-pyridylmethylamine) [35]. L-Tyr, also, in combination with the Vitamin B_6-amino acid Schiff base builds a

monomeric [Cu(5′-phosphopyridoxylidene-DL-Tyr)(H_2O)] complex [36]. The bridging carboxylate mode described as μ-(κ^3N, O;O') binds to the another Cu atom forming Cu—O—C—O—Cu link and causes a polymeric nature of the complex *catena*-(μ_2-N-Salicylidene-L-Tyr)-copper(II) [37].

As it was shown by us, the square pyramid geometry is preferred in Cu(II) complexes with L-tyrosine and its derivatives. It was found that, in [Cu(L-Tyr)$_2$X] and [Cu(L-Tyr)(diamine)X] units the apical position is favored by the water molecule [18, 23-25] and hardly ever is it replaced by NO_3^- [30] or perchlorate ion in [Cu(Ph-Tyr)(L)(ClO_4)] [31] and [Cu(hista)(L-Tyr)(ClO_4)] [38] (hista = histamine) or ethylamine [26].

In most cases, the interaction of L-tyrosine or its derivatives with copper(II) ions leads to the formation of square pyramidal complexes, what seems to be favored. However, four- or hexa- coordinated complexes, consisting of L-Tyr or its modifications, are also reported. Square planar geometry is created by L-tyrosinato O and N atom donors and N atoms of heterocyclic bases in [Cu(2,2'-bpy)(L-Tyr)]$ClO_4 \cdot 2H_2O$ [39] and [Cu(Fc-Tyr)(L)]$\cdot ClO_4$ [31] complexes (Fc = ferrocene, L = phen, dpq = dipyrido[3,2-d:2',3'-f]quinoxaline, dppz, nip = 2-(naphthalene-1-yl)-1H-imidazo[4,5-f][1,10]phenanthroline). Square planar geometry around Cu^{2+} ions is found in the salicylidene-L-tyrosinato complex of formulae K[CuL(Ac)]$\cdot H_2O$ [40, 41] and with hydroxyl dipeptide as L-seryl-L-tyrosine [42], which were synthesized as polycrystalline powder and widely physicochemically studied.

Among two six-coordinate crystalline L-tyrosinato complexes of formulae [Cu_2(L-Tyr)$_2$(NO_3)(4,4'-bpy)(H_2O)$_2$]$_n$ [43] and [Cu((N-pyridin-2-ylmethyl)-L-Tyr)$_2$]$\cdot 2H_2O$ [44], the first compound is a chiral two-dimensional coordination polymer consisting of [Cu_2(L-Tyr)$_2$(NO_3)(4,4'-bpy)(H_2O)$_2$]$_n$ units [43] joined by bridging oxygen carboxylate atoms forming μ-(O; O') mode.

In living organisms, the degradation of pheomelanin gives biomolecule 3-amino-L-tyrosine. Thus, it's protonation as well as the coordination behavior towards Cu(II) ions depending on pH values were performed via spectroscopic and potentiometric methods [45]. $[Cu(H_2A)]^{2+}$ complex is formatted at pH = 3.7 in concentration *ca.* 30 mol dm^{-3} as a first species. The monomeric $[Cu(HA)]^{+}$ and the dimeric $[Cu_2A_2H]^{+}$ entities are formed as a consequential complexes cations in the lower acidity, 4.3 - 5.0 pH range. But, the most stable dimeric $[Cu_2A_2]$ species formation starts with maximum concentration of *ca.* 90% found between 5.5 to 8.5 pH value. Finally, the anion $[Cu(A_2)]^{2-}$ complex is formed at pH = 10 in low concentration.

As we presented above L-tyrosine is a very flexible ligand and its coordination behavior, especially with Cu(II) bio-ions, arouses interest. The incessant studies of L-tyrosinate anions interactions with metal ions lead to the understanding of the process of complex formation and the stability of L-tyrosinato complexes as solid state and, also, in protic and aprotic solvents. We have undertaken the study of the Cu-L-tyrosine system to understand i) the influence of co-ligands on the physicochemical properties of the complex and ii) the biological characteristics of the species as it must be underlined that the biological. The biological synthesis pathways of neurotransmitters, hormone of thyroid and melanin are strongly dependent on the L-tyrosine concentration in blood. The complexation of the bio-availability metal ions by this amino acid could be one of the factors decreasing of concentration of free L-tyrosine in cellular fluids.

In the procedure of synthesizing new metal-L-tyrosine complexes we applied Zn^{2+}, Cu^{2+}, Ni^{2+}, Co^{2+} ions and biomolecules as co-ligands *i.e.* L-carnitine (L-car), salicylic (Sal) and acetylsalicylic (AcSal) acids, indole (Ind) and 7-azaindole (7-AzInd). Finally, we synthesized copper(II) L-tyrosinato complex as crystals of formula $[Cu(L\text{-}Tyr)_2(H_2O)]\cdot H_2O$ (**1**) by applying various metal ions and co-ligands. In this work we structurally characterized

the complex **1** by X-ray diffraction (SCXRD), spectroscopic methods as vibrational FT-IR, FT-Raman, electronic NIR-vis-UV, electron paramagnetic resonance (EPR) together with analysis of the magnetic susceptibility of the metal center interaction.

Experimental section

Chemicals, complex synthesis

All chemicals were of reagent grade and used as received. Hydrates of $CuCl_2 \cdot 2H_2O$, $Cu(NO_3)_2 \cdot 3H_2O$, $CuSO_4 \cdot 7H_2O$ and L-tyrosine disodium salt hydrate, L-carnitine hydrochloride, salicylic and acetylsalicylic acids, were purchased from Sigma-Aldrich. Dimethyl sulfoxide (DMSO) and methanol (MeOH) for spectroscopy used for recording the electronic and EPR spectra as well in biological studies were obtained from Fluka. Dichloromethane (CH_2Cl_2) comes from Merck.

A total of 10 mL of a 0.1M aqueous solution of Cu^{2+} ions was slowly mixed with 20 mL 0.1M aqueous solution of L-carnitine hydrochloride. 10 mL of a 0.1M aqueous solution of L-tyrosine disodium salt was added dropwisely To the blue clear mixture. 4 mL of dichloromethane was added to the obtained turquoise clear mixture and the mixture was continuously agitated. After 1 day, the resulting solution was filtered and the filtrate was left to evaporate slowly at room temperature. Navy crystals of complex **1** were obtained within 3 days. They were filtered, washed with water and one of them was X-ray characterized. Also, crystals of complex **1** crystalized from the mixture formed with molar ratio 1:1:1 by aqueous solution of $CuCl_2$ and methanol solution of salicylic or acetylsalicylic acids and L-tyrosine disodium salt in aqueous solution and 0.1 M concentration of each reagents. Anal. Calcd for $C_{18}H_{24}N_2O_8Cu$ (MW = 459.93): C, 47.01; H, 5.26; N, 6.09; Cu, 13.82. Found : C, 46.85; H, 5.03; N, 6.30; Cu, 13.45.

X-ray Crystallographic studies

The crystal structure of $[Cu(L\text{-}Tyr)_2H_2O]\cdot H_2O$ (**1**) was determined using a single-crystal X-ray diffraction. The data were collected on a Xcalibur diffractometer operating in κ-geometry and equipped with a two-dimensional CCD detector. *Mo Kα* radiation (0.71073Å) was used. The data were collected in ω-scan mode with $\Delta\omega$ =1.0^o using CrysAlis CCD program. The CrysAlis. RED software version 1.170.32 (Oxford Diffraction) [46] was used for data processing. The structure was solved by direct methods and refined by the full-matrix least–squares method against F^2 by means of SHELX–97 program package [47]. Anisotropic displacement parameters were applied for all non-hydrogen atoms. The hydrogen atoms from the organic part, excluding those from hydroxyl groups, were generated geometrically and treated as riding atoms. The $U_{iso}(H)$ were constrained to be $1.2U_{eq}$ (carrier atom). Disordered water molecules with occupancy factor of 0.5 were located from the difference Fourier map. The hydrogen atoms from disordered molecules were not identified. Powder diffraction data (XRD) were collected in a reflection mode, in the Bragg-Brentano geometry using X'Pert PRO X-ray diffraction system. Figure S1 presents XRD patterns for $[Cu(L\text{-}Tyr)_2(H_2O)]\ H_2O$ (**1**). All peaks are indexed in the unit cell obtained from the single-crystal X-ray diffraction. The differences in relative intensity for some peaks originate from texture effects. The more disturbed is the intensity of 1 0 0 peak that is much higher compare to other peaks. Obtained powders are homogenous without the traces of different phases.

Physicochemical and Spectroscopic Studies

Elemental analysis for Cu^{2+} ions was performed by the ICP-AES method and that of CHN using the Kumpan method. The vibrational FT-IR spectra were taken for complex **1** and both ligands (L-tyrosine disodium salt hydrate and L-carnitine hydrochloride). FT-IR and FIR spectra over the range 4000–50 cm^{-1} were recorded in KBr pellets (0.5 wt. % mass) or Nujoll mulls using the Perkin–Elmer FTIR-2000 spectrophotometer with resolutions of 4 cm^{-1} and 2 cm^{-1}, respectively. The FT-Raman spectrum of **1** was measured on a Bruker MultiRam

spectrometer equipped with a Nd:YaG laser and a liquid N_2 cooled germanium detector with resolution of 2 cm^{-1} with co-addition of 256 scans. The NIR–vis–UV electronic spectra were obtained on a Cary 500 Scan Spectrophotometer over the range 5000–50000 cm^{-1} with a measure step of 10 cm^{-1} at 293 K. Solid-state reflectance spectra were measured for **1**, L-tyrosine disodium salt with identical parameters as a baseline of white reference sample. Absorbance spectra were recorded for **1** and ligand in DMSO with concentration of $9{,}83\times10^{-4}$ M (**1**) and $1{,}042\times10^{-2}$ M (L-Tyr salt), respectively. Additionally, the absorbance spectra of **1** in FBS, RPMI-1640 and RPMI-1640 supplemented with 10% PBS (ingredients of solutions in biological tests) were collected.

The spectra of complex **1** were enhanced by using the variable digital method [48-52]. The method uses a single convolution of the spectral points measured at equal steps with a filter function a(n) :

$$T(k) = \sum_{n=-N}^{N} a(n) \times f(k-n)$$

where : $a(n) = (2\alpha + 1) / (2N + 1) - 2\alpha \,|n|\, / N(N+1)$

N – actual number of the sum component ($-N < n < N$) , T(*k*) is the filtered value in the k-th measured point, f – the unfiltered spectrum, N – the filter width and α is a real number determining the degree of the resolution enhancement. By varying α and N one can achieve different degrees of noise reduction, an increase of height and a decrease of width of the component bands. In order to obtain the approximate band positions for spectra of complex **1** we used : step = 20 cm^{-1}, α = 200 and N=30.

Fluorescence emission spectra of **1** dissolved in DMSO of 0.5, 0.25 and 0.125 mg/mol concentrations were carried out on LS50B Perkin Elmer spectrophotometer in the range 250-850 nm. Samples were prepared in 10 mm path length quartz cuvettes to avoid the inner-filter effect. The fluorescence intensity was measured with an excitation wavelength of 303 nm.

EPR spectra were measured using a Bruker Elexys E 500 Spectrometer equipped with NMR teslamerter (ER 036TM) and frequency counter (E 41 FRC) at X-band of solid state complex **1** at room and 77K temperatures. The experimental spectra were simulated using computer programs, DoubletExact (S=1/2) and CuDimer (S = 1), written by Dr. Andrew Ozarowski from NHMFL, University of Florida. Magnetic susceptibility of complex **1** in the temperature range from 1.7 to 300 K in a field of 500 mT and magnetization up to 5 T were measured with a Quantum Design SQUID magnetometer. The powder samples were pressed into pellets to avoid magnetic torquing. Diamagnetic correction ($-243 \cdot 10^{-6}$ emu·mol^{-1}) was calculated using Pascal's constants.

Results and discussion

L-carnitine, salicylic and acetylsalicylic acids are used as reagents in preparation of **1** but, none of them is included in a crystal structure. They play a catalytic function. The synthesis using only Cu^{2+} and L-tyrosine salts gave crystals of the coordination polymer $[Cu(L\text{-}Tyr)_2]_n$ described previously [20, 21].

Crystal structure

$[Cu(L\text{-}Tyr)_2(H_2O)]\cdot H_2O$ (**1**) crystalizes in the monoclinic $P2_1$ symmetry with relatively small unit cell accommodating two molecules of $[Cu(L\text{-}Tyr)_2(H_2O)]$ complex, V = 1046.4 (2)Å^3 and Z = 2. The crystal data, data collection and refinement results are presented in Table S1. The structure of $[Cu(L\text{-}Tyr)_2(H_2O)]$ complex is shown in Figure 1. Selected bond lengths and angles are listed in Table 1. Copper atom is coordinated by chelating carboxylate oxygen atoms (O(1), O(4)) and the amine nitrogen atoms (N(1), N(2)) from two L-tyrosinate anions and oxygen atom $O(1)_w$ of coordinated water molecule. The coordination sphere is described as a square pyramid with the corners of the CuN_2O_2 basal plane, occupied by chelating atoms and the apical position occupied by a water molecule. The side chain aromatic ring of L-tyr is placed approximately parallel to the basal plane of square pyramid. The coordination sphere may be extended to six-coordinated, taking into account the intramolecular cation-π interaction between the aromatic ring of the coordinated L-Tyr ligand and copper atom ($Cu^{2+}\cdots\pi$ distance equals 3.48 Å). Similar configuration of intramolecular stacking with distances 3.49 Å was found in $[Cu(L\text{-}Tyr)_2]_n$ [20-22] and other L-tyrosinato, L-phenolato or tryptophano Pd(II) and Cu(II) ions complexes, which consist of a characteristically bent aromatic ring [20-22, 26-31, 38, 53]. For **1** the $Cu^{2+}\cdots\pi$ distance is comparable to complexes listed above. The square planar geometry around Cu^{2+} is distorted, similar to the geometry around Pd^{2+} [53d] and Cu^{2+} [38, 53b] suggesting that aromatic ring in the vicinity of the metal coordination sphere may have an electronic effect on the central metal ion. On the other hand, the reactivity

of the aromatic ring may be disturbed by the metal center. Due to this weak bonding aromatic groups of amino acids in proteins may act as important binding sites for the copper ion. It has been shown that L-tyrosine side chain is coordinated to the Cu^{2+} ion in the active site of the enzyme occupying an axial position in the square-pyramidal geometry around copper center [53g-h].

The Cu-N_{amine} bonds (N(1)-Cu 1.99(1), N(2)-Cu 1.98(1)Å) are comparable with Cu-$O_{carboxylate}$ distances (Cu-O(1) 1.97(1) Cu-O(4) 1.95(1)Å) and are quite similar to those found in $[Cu(L\text{-}Tyr)_2]_n$ and other Cu(II) complexes [18, 20-22, 53i]. The distance from Cu(II) to apical $O(1)_{water}$ oxygen is longer 2.347 (4) Å but within the range of 2.2-2.9 Å known for the axial Cu-O bond lengths [54]. The angular parameter of the degree of trigonality defined as $\tau = (\beta - \alpha) / 60$ [55]; where α = N(1)–Cu(1)–O(4) (170,6(2) deg), β = N(2)–Cu(1)–O(1) (177,4(2) deg.), equals 0.113, and evidences a small distortion of the basal plane. The values of τ parameter, for all five-coordinated copper(II) L-tyrosinato and its derivative complexes deposited in the Cambridge Structural Database (CSD) [56], are collected in Table 2. In addition, it is noteworthy that this amino-acid forms five-coordinate complexes with only square planar geometry around Cu(II) ions. The obtained value 0.113 for **1** is nestled between 0,125 and 0,0813 calculated for $[Cu(Ph\text{-}Tyr)(phen)(ClO_4)]$ [31] and $[Cu(IP)(L\text{-}Tyr)(H_2O)]ClO_4 \cdot H_2O$ [28], respectively.

The asymmetric unit contains one symmetrically independent molecule of the complex and water disordered over two positions with probability 0.5. Crystal packing is presented in Fig. 2. The complete list of hydrogen bond interactions is presented in Table 4. Centers separated by the distance of 6.454 Å are joined by N(1)—H···O(2)^{v} and $O(1)_w$—H···O(2)^{iii} interactions. Additionally, $O(1)_w$ atom of coordinated water is a donor atom in $O(1)_w$—H···O(6)^{iv} bond to hydroxyl oxygen atom. Both phenolate oxygen atoms O(6) and O(3) act as donors and are involved in hydrogen bonds with uncoordinated carboxylate O5 and O2 atoms.

Hydroxyl oxygen O(6) atom is a donor in O(6)—H···O(2)^{ii} interaction with uncoordinated O(2)^{ii}. Whereas, hydroxyl oxygen O(3) atom from L-Tyr interacts via the O(3)—H···O5^{i} bond with the uncoordinated oxygen atom O5 from the carboxylate group of second L-Tyr anion joining two distant centers.

As it is seen in Table 4, carboxylate oxygen atoms act as acceptors in hydrogen bonds formation, O(2) is engaged in three bonds, O(5) in two and O(4) only in one hydrogen bond, whereas, carboxylate O(1) atom does not form any hydrogen interactions. Some hydrogen bonds may also be present between disordered water molecules since the closest O2···O2$^{(i)}$ distance is equal to 3.06 Å.

Due to several hydrogen bond interactions complex polymorphic structures are formed. Neighboring Cu(II) centers with $Cu^{2+}\cdots Cu^{2+}$ distance equal to 5.998(1) Å are directly connected by N(1)—H···O(4)^{vi} hydrogen bonds; donor and acceptor atoms are coordinated to two adjacent centers and together with N(2)—H···O(5)^{vi} interactions form tapes of [Cu(L-Tyr)$_2$(H$_2$O)] expanding along b direction, see Fig. 3. It must be emphasized that O(4) and O(5) atoms are from one molecule of amino acid. In the crystal structure of [Cu(L-Tyr)$_2$]$_n$ [21, 22] hydrogen bonds of similar strength are formed by N(1A)—H(1A1)···O(2A) and N(1B)—H(1B2)···O(2B) and involve oxygen atoms. However the acceptors of hydrogen are from two independent L-Tyr anions. The donor to acceptor distances are slightly shorter for **1** in comparison with distances found for [Cu(L-Tyr)$_2$]$_n$ [21, 22] (2.961 Å and 2.904 Å for **1** and 3.072(2) Å and 3.080(3) Å for [Cu(L-Tyr)$_2$]$_n$).

The chains based on the N(1)—H···O(4)^{vi} and N(2)—H···O(5)^{vi} hydrogen bonds propagate along b axis and join copper centers laying in the distance of 5.998(1) Å. The 5.998(1) Å and 6.454(1) Å distances are the shortest possible immediate contacts between metal centres and it is highly probable that hydrogen bonded chains are pathways for magnetic interactions (*vide infra*). The other distances between Cu(II) ions are definitely

longer and equal to 9.936 Å and 11.967 Å and should be definitely rejected as pathways of magnetic exchange (Fig. 4).

FT-IR vibrational and FT-Raman spectra

The spectrum of **1** exhibits a well seen band at 3482 cm^{-1}. This band is not found in FT-IR spectrum for $[Cu(L\text{-}Tyr)_2]_n$ complex [21]. Therefore, it should be attributed to the OH stretching vibrations and confirm the presence of water molecules in the crystal structure of **1**. Whereas, the OH stretching modes of phenolate rings generate a band found at 3372 cm^{-1} in a spectrum of **1**. In the spectral range 3400-2700 cm^{-1} several modes of ν_{as}, ν_s NH, ν CH and intramolecular O—H···N hydrogen bond between COOH and NH_2 groups vibrations as overlapped bands are observed [57-58]. The ν_{as} and ν_{sym} (NH_2) vibrations generate bands at 3284 cm^{-1} and 3264 are slightly downshifted in comparison with 3310 and 3295 cm^{-1} found for $[Cu(L\text{-}Tyr)_2]_n$ [21]. The Raman spectra of **1** exhibits bands at 3065, 3042, 3019 and 2967, 2948 and 2928 cm^{-1}.

In spectrum **1** regions 1700-1540 cm^{-1} and 1470-1350 cm^{-1} are the most interesting from the coordination perspective. In these spectral ranges the bands assigned as ν_{as} and ν_{sym} vibrations of COO^- groups arise. Strong and broad absorption found at 1700-1540 cm^{-1} consist of 1653, 1620, 1609, 1602 and 1585 cm^{-1} overlapping bands of ν_{as} C=O, scissoring NH_2 vibrations and, also, C-C vibrations of aromatic L-tyrosinato residues [57, 59]. In Raman spectra two strong bands were found at 1615 and 1591 cm^{-1}. The ν C-C and bending HC-CC vibrations in ring generate the very strong band at 1502, 1513 and 1515 for L-tyr salt, $[Cu(L\text{-}Tyr)_2]_n$ and complex **1**, respectively [57, 60]. One very weak band has been found at 1513 cm^{-1} in Raman spectra. The subsequent range 1470-1300 cm^{-1} presents weakly bands at 1456, 1444, 1406, 1380, 1352, 1329, 1311 cm^{-1}, which have their equivalents in reported previously spectra for $[Cu(L\text{-}Tyr)_2]_n$ [21] (Fig. S1). For both complexes the observed modes between 1470 cm^{-1} and 1375 cm^{-1} are the results of splitting band at *ca.* 1430 cm^{-1} found for pure L-tyrosine

salt and arise by stretching C-C and CO and bending HCC, HCH, HCN vibrations. The spectrum of **1** exhibits four bands, whereas six bands are found for $[Cu(L\text{-}Tyr)_2]_n$. Especially, the differences in the number and positions of the bands are the results of carboxylate monodentatelly and bridging coordinated carboxylate group in **1** and $[Cu(L\text{-}Tyr)_2]_n$, respectively. The involvement of oxygen atoms in several hydrogen bonds is an additional factor, what explains the differences in the spectra of these compounds. Whereas, bending HCN, HNC, HC-C_{ring} and HO-C_{ring} and ν C-C_{ring} vibrations appear as weak bands found at 1365, 1352, 1329 cm^{-1}. It stays in a good correlation with quantum chemical calculations for conformers of L-tyrosine [57]. The spectral range 1290-1210 cm^{-1} shows two very intensive and one weak bands at 1270, 1247 and 1212 cm^{-1}, which correspond to the band at 1271, 1242 and 1213 cm^{-1} observed in Raman spectrum. The energy values of those modes are reduced to *ca.* 10 cm^{-1} to lower energy in comparison with L-Tyr salt (Fig. S2). The bands are the result of several modes combination *ie.* ν (CC), τ(HCCC), ϕ (HCC), ν (OC) and ϕ (HNC) [57].

NIR-Vis-UV Electronic Spectroscopy and Fluorescence Spectra

The N and O atoms of L-tyrosine molecules and water O atom create five-coordinated enviroment around Cu(II) ion (d^9 system) and [CuN_2O_2O'] chomophore. The value of τ parameter 0.113 suggests the very small distortion towards trigonal bipyramid (TB). The single, broad and almost symmetrical band found with maximum at 15700 cm^{-1} is characteristic for square pyramidal (SP) geometry of the crystal filed around copper(II) centre (Fig. 5). It is atributable for the *d-d* transition of the distorted SP and it is very convergent to the spectra for SP enviroment found for $[Cu(L\text{-}Arg)_2(H_2O)]_2\cdot(pma)\cdot 3H_2O$ (L-Arg = L-arginine, pma^{4-} = pyromellitate) [61] and $[Cu(L\text{-}Tyr)_2]_n$ [21]. In **1**the distortion is a little bit smaller than in $[Cu(L\text{-}Arg)_2H_2O]^{2+}$ cation complex (0,1635 (CuA); 0,1483 (CuB)) as well as $[Cu(L\text{-}Tyr)_2]_n$ (0.19) and the maximum is red-shifted *ca.* 1100 cm^{-1} for **1**. In SP crystal field the one-electron ground state configuration follows as $d_{x2-y2} > d_{z2} > d_{xy} > d_{xz} \approx d_{yz}$ [62], what indicates

three *d-d* electronic transitions. The filtration of 10000 – 20000 cm^{-1} spectral range discloses five bands with energies 11440, 12620, 14880, 15800 and 19950 cm^{-1} (Fig. 6). The first two of them are associated with L-tyrosine overtones (Figs. 5 and 6), whereas, subsequent should be correlated with crystal field transitions. The single *d-d* band consists of three isolated oneself components. The spectrum is interpreted according to C_{4v} symmetry and those components are ascribed to the transition $^2B_1(d_{x2-y2}) \rightarrow {}^2A_1$ (d_{z2}), $^2B_1 \rightarrow {}^2B_2$ (d_{xy}) and $^2B_1 \rightarrow {}^2E$ ($d_{xz} \approx d_{yz}$) (Fig. 6) [62-65]. As in the case of the reflectance spectrum, the absorbance spectra exhibit intensive, symmetrical single band at *ca.* 16400 cm^{-1} (Fig. S3). This principal absorption with value of $\varepsilon = 80\ L^3 \cdot mol^{-1} \cdot cm^{-1}$ is characteristic for five-coordinated Cu(II) ion complexes as well as for other L-tyrosinato copper(II) spectra recorded in solvents *i.e.* DMF-tris-HCl buffer [31], aqueous [24], and also for two other aromatic aminoacids as L-phenylalanine and L-tryptophane [66, 67]. The spectrum of **1** recorded after 5 months preserves its shape, maximum and intensity. So, complex **1** is stable over time and coordination sphere is unchanged by the DMSO molecules. Preserving the pyramidal geometry around Cu(II) ion in DMSO solution is one of the most important observation in the context of biological research.

The fluorescence emission spectra show the emission wavelength at 14900 and 16400 cm^{-1}. The highly sensitive and selective peak at 16400 cm^{-1} (620 nm) is characteristic for L-Tyr [69] (Fig. S4)).

EPR Spectra

The EPR spectra of **1** were recorded at X-band on powder sample at 295 and 77 K (Fig. 7) and also on glassy DMSO solutions at 77 K (Fig. 8). The solid-state samples clearly indicate an axial S = 1/2 species spectrum. Diagonal components of g tensor, $g_{II} = 2.236$ and $g_{\perp} = 2.063$, obtained by simulation of the solid state spectrum, adopt the relation $g_{II(z)} > g_{\perp (x, y)}$ corresponding to d_{x2-y2} orbital of unpaired electron ground state, in agreement with the square-pyramidal geometry of Cu(II) complex. The EPR spectral parameters are very close to those

obtained on the basis of monocrystal EPR measurements of $[Cu(L\text{-}Tyr)_2]_n$ ($g_{||}$=2.2414 and $g_{\perp}$=2.0584) [22]. The EPR parameters of the monomeric species observed in the DMSO frozen solution $g_{||}$ = 2.250, $g_{\perp}$= 2.055,and $A_{||}$ = 180 G, are typical for N_2O_2 donor set from two bidentate L-tyrosine ligands coordinated in Cu(II) xy plane. Surprisingly, the same spectrum of the DMSO frozen solution exhibits the lines associated with S = 1 species. It is clearly demonstrated by the presence of forbidden ($\Delta M_S = \pm 2$) resonance transition at half-field, displaying a 7-line splitting structure from hyperfine interaction with two copper nuclei (I(Cu) = 3/2) within the dimeric unit. The hyperfine coupling parameter, $A_{||}$ = 85 G, is equal to half the value which characterizes the monomeric Cu(II) complex. The same splitting is observed at allowed low field $\Delta M_S = \pm 1$ transition superimposed on the lines of dominant monomeric species. The simulation of EPR spectrum using S=1 spin Hamiltonian gave $|D| = 0.0468$ cm^{-1}, $g_{||}$ = 2.238, $g_{\perp}$ = 2.06 and $A_{||}$ = 85 G what suggests that Cu(II) pair is involved in a very week exchange coupling [70]. According to the crystal structure data, there are two oxygens, phenolic and carboxylic, which are not coordinated to Cu(II) ion and may participate in the bridging of Cu(II) ions at long distance. The Yamauchi and co-workers reported that the copper(II) complexes of Tyr-containing dipeptides dimerized through the phenoxide bridge at pH 8-11 [70a-b]. Assuming dipole-dipole nature of the obtained D parameter the Cu···Cu distance may be estimated [70c] as close to 4 Å.

Magnetic Measurements

The magnetic susceptibility of **1** (Fig. 9) shows the Curie–Weiss behavior virtually in the whole temperature range with a Weiss constant θ = –0.40 K and a magnetic moment of 1.87 μ_B. The effective magnetic moment is constant at 12–300 K (1.85–1.87 μ_B) and below 12 K increases to 1.94 μ_B at 1.72 K. The negative value of θ usually indicates an antiferromagnetic exchange coupling, but it is important to note that after subtracting temperature independent

paramagnetism from the raw experimental data, the parameter changes the sign (see further discussion).

The increase of the effective magnetic moment at low temperatures suggests the existence of weak intermolecular ferromagnetic interactions. Taking into account the structural features, structures with two competing interactions cannot be excluded. Although, there is no direct metal-metal bridges, the copper ions are connected through the elaborate system of hydrogen bonds (Figures 2 and 3). They provide potential magnetic superexchange pathways, often quite effective in copper complexes [71] (Fig. 4). Looking for possible magnetic interactions we find Cu(II) double chains running along the *b* axis. The ions in adjacent chains are shifted from one another by half the shortest Cu···Cu distance. Such an arrangement of magnetic ions is called a double triangular chain [72] or, in case of antiferromagnetic interactions, a frustrated double chain [73]. [Cu(L-Tyr)$_2$(H$_2$O)] units in the chains are linked through the double N—H···O hydrogen-bonds involving both the coordinated and free carboxylate-oxygen atoms. Possible interactions transmitted in this way should not be very weak because: (i) N—H···O bonds came under the strongest hydrogen bonds [74], (ii) the atoms involved in the bonds (directly or indirectly) belong to the basal planes of the coordination polyhedra. The adjacent planes N1N2O1O4 are strictly parallel, but shifted from each other by 1.024 Å. Each copper ion is linked to two ions in the adjacent chain by single hydrogen bonds O1*W*—H1*W*···O2. These contacts are probably very weak, attaching the uncoordinated oxygen atom of the carboxylate group with the apical water molecule in the apical-basal mode.

The magnetic susceptibility data were fitted using a high-temperature series expansion (HTSE) derived from the one-dimensional Heisenberg model for S = ½, based on the Padé approximant technique [75-76] :

$$\chi = (Ng^2\beta^2 / 4kT)\,[N/D]^{2/3} + N\alpha$$

in which $N = 1.0 + 5.7979916y + 16.902653y^2 + 29.376885y^3 + 29.832959y^4 + 14.036918y^5$, $D = 1.0+2.7979916y + 7.0086780y^2 + 8.6538644y^3 + 4.5743114y^4$, and $y = J/4kT$ (adjusting the equation to $H = -JS_1S_2$ convention). $N\alpha$ stands for the temperature independent paramagnetism. A very good agreement between the simulated and experimental susceptibility, even at very low temperatures, (Fig. 9), was achieved with $J = +0.30$ cm^{-1}, $N\alpha = 61\cdot10^{-6}$ emu/mol, and g fixed as 2.1207 according to the average value obtained by EPR measurements, $R = \Sigma[(\chi T)_{exp} - (\chi T)_{calc}]^2 / \Sigma[(\chi T)_{exp}]^2 = 2.8\cdot10^{-5}$ (76 points). Completely identical results were obtained using the 9th order HTSE for a two-leg Heisenberg spin-ladder model (Eq. 14 in Ref. [77], not presented here because of their complexity), assuming $J_\perp$ (rungs of a ladder) = 0. No significant improvement of the susceptibility fit was achieved after the introduction of an additional coupling parameter, zJ', to account for the possible interchain interactions through O1*W*—H1*W*···O2—C2—O1 bridges (Figure 2b). The *Na* parameter is very close to value of $60\cdot10^{-6}$ emu/mol, which is commonly assumed in the literature. It deserves to be noted that the exchange constant J is positive, despite the negative value of the Weiss constant θ. This effect is due to temperature independent paramagnetism, and, after subtracting $N\alpha$ from the measured susceptibility, $\mu = 1.83\ \mu_B$ and $\theta = +0.51$ K are obtained.

Since it is not possible to calculate field dependent magnetization within the above model, we have tried to ignore very weak exchange interactions, treating the system as a set of isolated Cu(II) ions and leaving the rest of the parameters (g, $N\alpha$) unchanged. The $M(B)$ dependence calculated for various external fields is drawn in Fig. 10 as a solid line and fits the experimental data pretty well.

Magnetic interactions transmitted via O—H···O hydrogen bonds have been detected in dozens of compounds, some magnetostructural relationships were also found [71, 78]. Much less common are the arrangements with nitrogen donor atoms. Table 4 compiles the

Cu(II) compounds with the N—H···O bridging mode, where the exchange integrals have been determined from the magnetization data [79]. No clear magnetostructural trends have been observed (also among the geometric parameters not listed in the Table) but it is worth to mention that the basal-basal type configuration of the CuN_2O_2O' coordination polyhedra favors ferromagnetic interactions. This is rather unexpected, especially in light of the results obtained previously for the compounds with O—H···O hydrogen bonds [71, 80], where "a such condition has been shown to be crucial for the system to exhibit antiferromagnetic interactions" [80b].

Conclusion

In summary, we have presented a five-coordinated copper(II) L-tyrosinato complex, $[Cu(L\text{-}Tyr)_2(H_2O)]\cdot H_2O$ (**1**), and characterization of its crystal structures, spectroscopic as well as magnetic properties. The L-tyrosinate anions chelate copper(II) ions and together with water molecules form square pyramidal (SP) environment around metal centres. The monomer $[Cu(L\text{-}Tyr)_2(H_2O)]$ complexes are directly connected by N(1)-H···O(4)^{vi} and N(2)-H···O(5)^{vi} hydrogen bonds. These interactions form tapes of $[Cu(L\text{-}tyr)_2(H_2O)]$ in which joined Cu^{2+} centers are distanced of 5.998(1) Å. The chain based on N(1)-H···O(4)^{vi} and N(2)-H···O(5)^{vi} hydrogen bonds is one of the magnetic superexchange pathways of a weak ferromagnetic interaction between neighboring copper(II) ions. The EPR parameters of the monomeric species observed in the DMSO frozen solution are typical for N_2O_2 donor set. Also, in the DMSO frozen solution the 7-line splitting structure from hyperfine interaction with two copper nuclei (I(Cu) = 3/2) within the dimeric unit were found. In the reflectance spectrum, the single *d-d* band is composed by $^2B_1(d_{x2-y2}) \rightarrow {}^2A_1$ (d_{z2}), $^2B_1 \rightarrow {}^2B_2$ (d_{xy}) and $^2B_1 \rightarrow {}^2E$ ($d_{xz} \approx d_{yz}$) transition with the ground state $^2B_1(d_{x2-y2})$. The SP copper(II) geometry has been preserved in DMSO.

Acknowledgements

The work was financed by a statutory activity subsidy from the Polish Ministry of Science and Higher Education for the Faculty of Chemistry of Wrocław University of Technology. The fluorescence spectra were measured at Chemistry Department, University of California, Berkeley, during the A.W internship of TOP-500 Innovators Poland Program.

Appendix A. Supplementary data

Supporting Information. X-ray crystallographic data in CIF format for **1**, tables and supplementary figures. This material is available free of charge *via* the Internet at www.rsc.org/advances. Crystallographic data for **1** have also been deposited with the Cambridge Crystallographic Data Centre, and are available at www.ccdc.cam.ac.uk/data_request/cif under the deposition number CCDC-980662.

Table 1 Selected bond distances (Å) and angles (deg) in complex **1**

Distances			
Cu1—O4	1.946(4)	Cu1—N2	1.979(5)
Cu1—O1	1.972(4)	Cu1—N1	1.987(5)
Cu1—O1*W*	2.347(4)		
Angles			
O4—Cu1—O1	94.1(2)	N2—Cu1—O1*W*	85.9(2)
O4—Cu1—N2	83.5(2)	N1—Cu1—O1*W*	99.8(2)
O1—Cu1—N2	177.4(2)	C2—O1—Cu1	113.0(4)
O4—Cu1—N1	170.6(2)	C10—O4—Cu1	116.9(4)
N2—Cu1—N1	83.1(2)	C1—N1—Cu1	107.6(4)
N2—Cu1—N1	99.1(2)	C11—N2—Cu1	111.5(4)
O4—Cu1—O1*W*	89.4(2)	C2—C1—C3	110.9(5)
O1—Cu1—O1*W*	95.3(2)	C13—C12—C11	116(5)

Table 2 The chromophores, values of α, β angles (deg) and value of τ parameter for L-tyrosinato and its derivatives five-coordinated copper(II) complexes

	Complex	Chromophore	Angles : α ; β	$\tau = (\beta - \alpha) / 60$ [55]
1.	$[Cu(2,2'\text{-bpy})(L\text{-Tyr})(H_2O)]Cl\cdot 3H_2O$ [23]	N_2NOO'	174.0 ; 151.8	0.370
2.	$[Cu(2,2'\text{-bpy})(I_2tyrOH)(NO_3)]\cdot CH_3OH$ [30]	N_2NOO'	174.8 ; 156.3	0.308
3.	$[Cu(2,2'\text{-bpy})(I_2tyrO^-)(H_2O)]\cdot 2H_2O$ [30]	N_2NOO'	177.1 ; 160.3	0.280
4.	$[Cu(2,2'\text{-bpy})(L\text{-Ityr})(H_2O)]NO_3\cdot CH_3OH\cdot H_2O$ [29]	N_2NOO'	173.7 ; 159.9	0.230
5.	$[Cu(L\text{-Tyr})(phen)(H_2O)]ClO_4\cdot 2.5H_2O$ [24]	N_2NOO'	Cu(1) 173.7;161.8	0.198
			Cu(2) 170.8 ; 160.3	0.175
6.	$[Cu(L\text{-Tyr})_2]_n$ [18, 20, 21]	N_2O_3	179.2 ; 167.5 [5]	0.195
			179.32;167.75 [6]	0.193
			179.3;168.0 [3]	0.188
7.	$[Cu(hista)(L\text{-}I_2tyrO^-)(H_2O)]_2\cdot 2H_2O$ [29]	N_2NOO'	Cu(2) 173.6 ; 163.6	0.166
			Cu(1) 165.9 ; 164.6	0.022
8.	$[Cu(Ph\text{-Tyr})(phen)(ClO_4)]$ [31]	N_2NOO'	176.08 ; 168.56	0.125

9.	$[Cu(L\text{-}Tyr)_2(H_2O)]\cdot H_2O$ (this work)	N_2O_2O'	170.6 ; 177.4	0.113
10.	$[Cu(IP)(L\text{-}Tyr)(H_2O)]ClO_4\cdot H_2O$ [28]	N_2NOO'	170.63 ; 165.74	0.081
11.	$[Cu(L\text{-}Tyr)(5,6\text{-}dmp)(H_2O)]ClO_4$ [27]	N_2NOO'	Cu(2) 166.62;163.95	0.044
			Cu(1) 166.19;164.30	0.032
12.	[Cu(L-Tyr-hist)] [32]	N_3O_2	177.0 ; 174.8	0.037
13.	$[Cu(hista)(L\text{-}Tyr)(ClO_4)]$ [31]	N_2NOO'	170.1 ; 168.6	0.025

L-Tyr = L-tyrosine; 2,2'-bpy = 2,2'-bipyridine; phen = 1,10-phenanthroline; 5,6-dmp = 5,6-dimethyl-1,10-phenanthroline; IP = imidazol[4,5-*f*][1,10] phenanthroline; L-Ityr = 3-iodo-L-tyrosine ; hista = histamine ; I_2tyr = 3,5-diiodo-L-tyrosine ; L-Tyr-hist = L-tyrosyl-L-histidine ; Ph-Tyr = L-phenylalanine-L-tyrosine

Table Hydrogen-bonding interactions in the crystal structure of **1** [a]

D—H···*A*	*d*(*D*—H) / Å	d(H···*A*) / Å	*D*(*D*···*A*) / Å	<*D*HA / deg
O3—H31···O5^{i}	0.98(2)	1.85(3)	2.713(6)	145(5)
O6—H61···O2^{ii}	0.90(2)	1.82(3)	2.692(7)	161(5)
O1*W*—H1*W*···O2^{iii}	0.96	1.84	2.795(6)	178
O1*W*—H2*W*···O6^{iv}	0.89	1.91	2.804(7)	180
N1—H1A···O2^{v}	0.90	2.25	3.117(6)	161
N1—H1B···O4^{vi}	0.90	2.10	2.961(6)	159
N2—H2A···O5^{vi}	0.90	2.02	2.904(7)	167

[a] Symmetry transformations used to generate the equivalent atoms :: (i) -*x*+1, *y*+1/2, -*z*+2; (ii) *x*-1, *y*, *z*; (iii) -*x*+1, *y*-1/2, -*z*+1; (iv) -*x*, *y*+1/2, -*z*+1; (v) -*x*+1, *y*+1/2, -*z*+1; (vi) *x*, *y*+1, *z*.

Table 4 The Cu(II) compounds with the N—H···O bridging mode and magnetization data

Compound	Topology	*d* (Cu···Cu) (Å)	*h*[a] (Å)	*J*[b] (cm^{-1})
$[CuL^1py]_2 \cdot 0.5H_20$ [79a]	4-coord, T_d / D_{4h}	3.993		–6.5
$[\{Cu(en)\}_2(\mu\text{-egta})] \cdot 4H_2O$ [79b]	equatorial-axial	5.781	1.521	–1.35
$[Cu(L^2)(Cl)(L^3)] \cdot H_2O$ [79c]	basal-basal	5.776	2.381	+0.21[c]
				+0.99[d]
$[Cu(L\text{-}Tyr)_2(H_2O)] \cdot H_2O$ (this work)	basal-basal	5.999	1.024	+0.30
$[CuL^4(N_3)]_2$ [79d]	basal-basal	5.700	2.104	+1.02

L^1 = 6-amino-1,3-dimethyl-5-((2-carboxyphenyl)azo)uracil; H_4egta = 3,12-bis(carboxymethyl)-6,9-dioxa-3,12-diazatetradecanedioic acid; L^2 = 2-aminomethylbenzimidazole; L^3 = L-isoleucinate; L^4 = 8-amino-4-methyl-5-azaoct-3-en-2-one; [a] the distance between the adjacent basal (equatorial) planes; [b] The J values were brought to the $-JS_iS_j$ convention; [c] Heisenberg dimer; [d] Ising chain

REFERENCES

1 S. Meyers, *Altern Med Rev.,* 2000, **5**, 64.

2 E.-J. Lee, P. J. Facchini, *Plant Physiology,* 2011, 1067.

3 (a) A. Nakagawa, H. Minami, J.-S. Kim, T. Koyanagi, T. Katyama, F. Sato, H. Kumag, *Nat. Commun.,* 2011, **2:326**, 1. (b) *Nat. Commun.,* 2012, **3:819**, 9.

4 P. Kovacic, R. Somanathan, *Oxid. Med. Longev.,* 2009, **2**, 181.

5 A. Slominski, M. A. Zmijewski, J. Pawelek, *Pigment Cell Melanoma Res.,* 2012, **25**, 14.

6 S.-Q. Li, N.-H. Hu, *Acta Crystallogr.,* 2011, **E67**, m884.

7 Shuo Zhang, Ning-Hai Hu, *Acta Crystallogr.,* 2009, **C65**, m7.

8 D. U. Miodragovic, G. A. Bogdanovic, S. M. Milosavljevic, M. J. Malinar, M. B. Celap, A. Spasojevic-de Bire, S. Macura, N. Juranic, *Enantiomer,* 2001, **6**, 299.

9 R. Dreos, G. Nardin, L. Randaccio, P. Siega, G. Tauzher, *Inorg. Chem.* 2004, **43**, 3433.

10 E. Gao, H.-Y. Li, Q.-T. Liu, *Acta Chim. Sinica,* 2005, **63**, 1225.

11 D.-Q. Li, J. Zhou, X. Liu, *Acta Crystallogr.,* 2007, **C63**, m371.

12 P. Kumar, A. K. Singh, J. K. Saxena, D. S. Pandey, *J. Organomet. Chem.* 2009, **694**, 3570.

13 M. S. Refat, S. A. El-Korashy, A. S. Ahmed, *J. Mol. Struct.,* 2008, **881**, 28.

14 G. A. Thakur, M. M. Shaikih, *Acta Poloniae Pharm. – Drug Res.,* 2006, **63**, 95.

15 Md. R. Islam, S. M. R. Islam, A. S. M. Noman, J. A. Khanam, S. M. M. Ali, S. Alam, M. Lee, *Mycobiology,* 2007, **35**, 25.

16 D. Van der Helm, W. A. Franks, *J. Am. Chem. Soc.,* 1968, **90**, 5627.

17 W. A. Franks, D. Van der Helm, *Acta Cryst.,* 1970, **B27**, 1299.

18 D. Van der Helm, C. E Tatsch, *Acta Cryst.,* 1972, **B28**, 2307.

19 C. A. McAuliffe, S. G. Murray, *Inorg. Chim. Acta.,* 1973, **7**, 171.

20 J. Weng, M. Hong, Q. Shi, R. Cao, A. S. C. Chan, *Eur. J. Inorg. Chem.,* 2002, 2553.

21 A. Wojciechowska, M. Daszkiewicz, A. Bienko, *Polyhedron,* 2009, **28**, 1481.

22 V. Padares-Garcia, R. C. Santana, R. Madrid, B. Baldo, A. Vega, E. Spodine, *J. Inorg. Biochem.,* 2012, **114**, 75.

23 X. Solans, L. Ruiz-Ramirez, A. Martinez, L. Gasque, R. Moreno-Esparza, *Acta Cryst.,* 1992, **C48**, 1785.

24 T. Sugimori, H. Masuda, N. Ohata, K. Koiwai, A. Odani, O. Yamauchi, *Inorg. Chem.,* 1997, **36**, 576.

25 P. R. Reddy, P. Manjula, *Chem. Biodiver.,* 2009, **6**, 71.

26 D. Kannan, M. N. Arumugham, *Inter. J. Inor. Bioinorg. Chem.,* 2012, **2**, 50.

27 S. Ramakrishna, V. Rajendiran, M. Palaniandavar, V. S. Periasamy, B. S. Srinag, H. Krishnamurthy, M. A. Akbarsha, *Inorg. Chem.,* 2009, **48**, 1309.

28 G. Qin, L. Xue-Yi, L. Qing-Bin, L. Sheng-Rong, M. Xue-Dan, F. Xiao-Long, *Chines J. Chem.,* 2007, **25**, 791.

29 F. Zhang, T. Yajima, H. Masuda, A. Odani, O. Yamauchi, *Inorg. Chem.,* 1997, **36**, 5777.

30 F. Zhang, A. Odani, H. Masuda, O. Yamauchi, *Inorg. Chem.,* 1996, **35**, 7148.

31 T. K. Goswami, S. Gadadhar, A. A. Karande, A. R. Chakravarty, *Polyhedron,* 2013, **52**, 1287.

32 H. Masuda, A. Odani, O. Yamauchi, *Inorg. Chem.* 1989, **28**, 624.

33 D. Van der Helm, S. E. Ealick, J. Burks, *Acta Cryst.,* 1975, **B31**, 1013.

34 A. Mosset, J. J. Bonnet, *Acta Cryst.,* 1977, **B33**, 2807.

35 T. Yajima, M. Okajima, A. Odani, O. Yamauchi, *Inorg. Chim. Acta.,* 2002, **339**, 445.

36 I. I. Mathews, H. Manohar, *Polyhedron,* 1991, **10**, 2163.

37 R. Hamalainen, M. Ahlgren, U. Turpeinen, M. Rantala, *Acta Chem. Scand. A.,* 1978, **32**, 235.

38 O. Yamauchi, T. Kohzuma, H. Masuda, K. Toriumi, K. Sato, *Inorg. Chem.* 1989, **28**, 4066.

39 O. Yamauchi, A. Odani, H. Masuda, *Inorg. Chim. Acta,* 1992, **198**, 749.

40 W. Shi, D. Chen, G. Wang, Y. Xu, *Appl. Magn. Reson.,* 2001, **20**, 289.

41 W.-L. Shi, D.-Y. Chen, *Acta Phys. Chim. Sin.,* 2001, **17**, 181.

42 T. Kolev, B. B. Koleva, M. Spiteller, *J. Coord. Chem.* 2008, **61**, 1897.

43 S. Zhang, N.-H. Hu, *Acta Cryst.* 2009, **C65**, m7.

44 X.-F. Li, R. Cao, Chin. *J. Struct. Chem.* 2009, **28**, 1439.

45 P. Sipos, T. Kiss, *J. Chem. Soc. Dalton Trans.* 1990, 2909.

46 CrysAlisCCD CrysAlis RED, Oxford Diffraction Ltd., Version 1.171.33.42, release 29-05-2009 CrysAlis171, 2009.

47 G. M. Sheldrick, *Acta Cryst.* 2008, **A64**, 112.

48 G. Bierman, H. Ziegler, *Anal. Chem.* 1986, **58**, 536.

49 J. Myrczek, *Spectrosc. Lett.,* 1990, **23**, 1027.

50 A. Wojciechowska, Z. Staszak, W. Bronowska, A. Pietraszko, M. Cieślak-Golonka, *Polyhedron*, 2001, **20**, 2063.

51 A. Wojciechowska, D. Dobrzyńska, J. Janczak, *Polyhedron*, 2012, **47***,* 118.

52 D. Dobrzyńska, L. B. Jerzykiewicz, M. Duczmal, A. Wojciechowska, *Polyhedron,* 2011*,* **30***,* 2684.

53 a)O. Yamauchi, A. Odani, M. Takani, J. Chem. Soc. Dalton Trans., **2002**, 3411. b) T. Yajima, R. Takamido, Y. Shimazaki, A. Odani, Y. Nakabayashi, O. Yamauchi, Dalton Trans., **2007**, 299. c) O. Yamauchi, A. Odani, S. Hirota, Bull. Chem. Soc. Jpn., **2001**, 74, 1525. d) M. Sabat, M. Jeżowska, H. Kozłowski, Inorg. Chim. ACTA 1979, 37, L511. f) H. Masuda, T. Sugimori, A. Odani, O. Yamauchi, Inorg. Chim. Acta 1991, 180, 73. g) M. C. J. Wilce, D. M. Dooley, H. C. Freeman, J. M. Guss, H. Matsunami, W. S. McIntire, C. E. Ruggiero, K. Tanizawa, H. Yamaguchi, *Biochemistry* **1997**, *36*, 16116. h) N. Ito, S. E. V. Phillips, C. Stevens, Z. B. Ogel, M. J. McPherson, J. N. S. Keen, K. D. Yadev, P. F. Knowles, *Nature* **1991**, *350*, 87. i) H. C. Freeman, *Ad. Protein Chem.* 1967, **22**, 257.

54 A. F. Wells, Structural Inorganic Chemistry; Oxford University Press: Oxford, U.K., 1975, 259.

55 A. W. Addison, T. N. Rao, J. Reedijk, J. Van Rijn, G. C. Verschoor, *J. Chem. Soc., Dalton Trans.* 1984, 1349.

56 I. J. Bruno, J. C. Cole, P. R. Edgington, M. Kessler, C. F. Macrae, P. McCabe, Soc. Hem., J. Pearson, R. Taylor, *Acta Cryst.* 2002, **B58**, 389. CSD version 5.31.

57 S. A. Siddiqui, A. K. Pandey, A. Dwivedi, S. Jain, M. Neeraj, *J. Chem. Pharm. Res.* 2010, **2**, 835.

58 Y. Inokuchi, Y. Kobayashi, T. Ito, T. J. Ebata, *Phys Chem.* 2007, **A 111**, 3209.

59 J. Garcia-Tojal, A. Barcia-Orad, J. Serra, J. Pizarro, L. Lezama, M. Arriortua, T. J. Rojo, *Inorg. Biochem.* 1999, **75**, 45.

60 A. Barth, Progr. Biophys. *Molec. Biology.,* 2000, **74**, 141.

61 N. Ohada, H. Masuda, O. Yamauchi, *Inorg. Chim. Acta.*1999, **286**, 37.

62 D. N. Sathyanarayana, Electronic Absorption Spectroscopy and Related Techniques, Universities Press, 2001, 1.

63 G. Murphy, C. O'Sullivan, B. Murphy, B. Hathaway, *Inorg. Chem.* 1998, **37**, 240.

64 G. Ondrejovic, A. Kotocova, D. Valigura, *Chem. Pap.* 2002, **56**, 169.

65 D. Dobrzynska, J. Janczak, A. Wojciechowska, K. Helios, *J. Molec. Struct.* 2010, **973**, 62.

66 A. K. Patra, T. Bhowmick, S. Ramakumar, M. Nethaji, A. R. Chakravarty, *Dalton Trans.,* 2008, 6966.

67 S. Y. New, X. Wu, S.-Q. Bai, L. L. Koh, T. S. A. Hor, F. Xue, CrystEngComm, 2011, 13 4228.

68 A. G. Griesbeck, J. Neudorfl, A. Kiff, Beilstein *J. Org. Chem.* 2011, **7**, 518.

69 M. S. Attia, A. O. Youssef, A. A. Essawy, *Anal. Methods.,* 2012, **4**, 2328.

70 a) O. Yamauchi, K. Tsujide, A. Odani, J. Am. Chem. Soc. 1985, 107, 659. b) R. J. W. Hefford, L. D. Pettit, J. Chem. Soc., Dalton Trans., 1981, 1331. c) D. L. Reger, A. Debreczeni, M. D. Smith, J. Jezierska, A. Ożarowski, *Inorg. Chem.* 2012, **51**, 1068.

71 C. Desplanches, E. Ruiz, A. Rodriguez-Fortea, S. Alvarez, *J. Am. Chem. Soc.* 2002, **124**, 5197.

72 S. Angelov, M. Drillon, E. Zhecheva, R. Stoyanova, M. Belaiche, A. Derory, A. Herr, *Inorg. Chem.* 1992, **31**, 1514.

73 R. Georges, J. J. Borras-Almenar, E. Coronado, J. Curely, M. Drillon, Magnetic chains. An overview of the models, in *Magnetism: Molecules to Materials. Models and Experiments*, ed. J. S. Miller and M. Drillon, Wiley-VCH 1, 2001, 1.

74 J. D. Dunitz, A. Gavezzotti, Cryst. Growth Des., 2012, **12**, 5873.

75 G. A. Baker, Jr., G. S. Rushbrooke, H. E. Gilbert, *Phys. Rev.* 1964, **135**, A1272.

76 O. Kahn, *Molecular Magnetism*, VCH Publishers, Inc., New York, 1993.

77 D. C. Johnston, M. Troyer, S. Miyahara, D. Lidsky, K. Ueda, M. Azuma, Z. Hiroi, M. Takano, M. Isobe, Y. Ueda, M. A. Korotin, V. I. Anisimov, A. V. Mahajan, J. L. Miller, arXiv:cond-mat/0001147, 2000.

78 (a) B. Le Guennic, N. Ben Amor, D. Maynau, V. Robert, *J. Chem. Theory Comput.* 2009, 5, 1506. (b) N. A. G. Bandeira, B. Le Guennic*, J. Phys. Chem. A,* 2012, **116**, 3465.

79 (a) E. Colacio, J. P. Costes, R. Kivekäs, J. P. Laurent, J. Ruiz, M. Sundberg, *Inorg. Chem.,* 1991, **30**, 1475. (b) E. Escriva, J. Server-Carrio, J. Garcia-Lozano, J. V. Folgado, F. Sapina, L. Lezama, *Inorg. Chim. Acta,* 1998, **279**, 58. (c) G. Carpinteyro-López, J. L. Alcántara-Flores, D. Ramírez-Rosales, R. Escudero, B. M. Cabrera-Vivas, S. Bernès, R. Zamorano-Ulloa, Y. Reyes-Ortega, ARKIVOC 2008 (v) 31. (d) M. S. Ray, A. Ghosh, R. Battacharya, G. Mukhopadhyay, M. G. B. Drew, J. Ribas, *Dalton Trans.,* 2004, 252.

80 (a) W. Plass, A. Pohlmann, J. Rautengarten, *Angew. Chem., Int. Ed.* 2001, **40**, 4207. (b) J. Tang, J. Sánchez Costa, A. Golobič, B. Kozlečvar, A. Robertazzi, A. V. Vargiu, P. Gamez, J. Reedijk, *Inorg. Chem.,* 2009, **48**, 5473.

81 H. D. Flack, *ActaCryst.,* 1983, **A39**, 876.

FIGURE CAPTIONS

Fig. 1. The structure of $[Cu(L\text{-}Tyr)_2(H_2O)]$ complex, dashed line stands for Cu(II)···π interaction with distance of 3.48 Å.

Fig. 2. (a) Crystal packing of **1** along *b* direction, disordered water accommodates empty voids in the crystal structure, (b) view perpendicular to *b* axis showing hydrogen bonds between neighboring centers, part of the ligands are not drawn for the picture clarity.

Fig. 3. Hydrogen bond interactions in $[Cu(L\text{-}Tyr)_2(H_2O)]\cdot H_2O$, part of the ligands are omitted for picture clarity.

Fig. 4. The projection of the crystal structure of $[Cu(L\text{-}Tyr)_2(H_2O)]\cdot H_2O$ with marked distances between copper centers.

Fig. 5. Polycrystalline electronic reflectance spectrum of **1** (—) and pure L-tyrosine disodium salt (- - -) .

Fig. 6. The effect of filtration process of reflectance spectrum for **1** (visible region) (step = 20 cm^{-1}, α = 200 and N=30).

Fig. 7. X-band EPR spectra of powdered complex **1** at 77K simulated using the parameters given in the text .

Fig. 8. EPR spectrum of the frozen DMSO solution of **1** together with the theoretical spectrum (sim), simulated using S=1 and the parameters given in the text. The stars indicate the signals due to monomeric S=1/2 complex from 1 (the first three lines are due to hyperfine interaction with one copper nuclei of parallel orientations). The above amplified fragment shows distinctly the hyperfine splitting due to two copper nuclei.

Fig. 9. Plots of reciprocal magnetic susceptibility, χ^{-1}, (◇) and effective magnetic moment, μ_{eff}, (Δ) versus temperature for [Cu(L-Tyr)$_2$(H_2O)]. The solid lines correspond to the best fit parameters (see text).

Fig. 10. Magnetization as a function of magnetic induction at 1.72 K. The line is the Brillouin function calculated for $S = ½$, $g = 2.1207$ (EPR average) and $N\alpha = 61 \cdot 10^{-6}$ emu/mol.

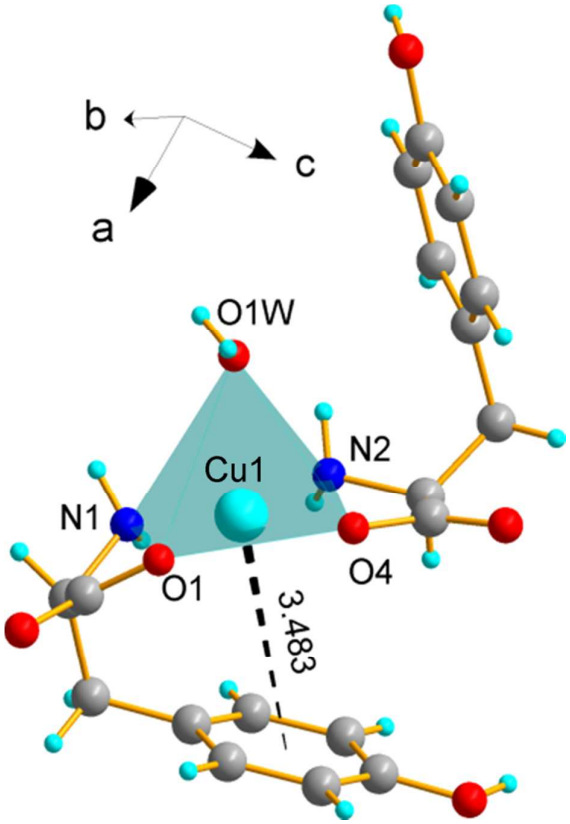

Fig. 1 The structure of $[Cu(L\text{-}Tyr)_2(H_2O)]$ complex, dashed line stands for Cu(II)···π interaction with distance of 3.48 Å

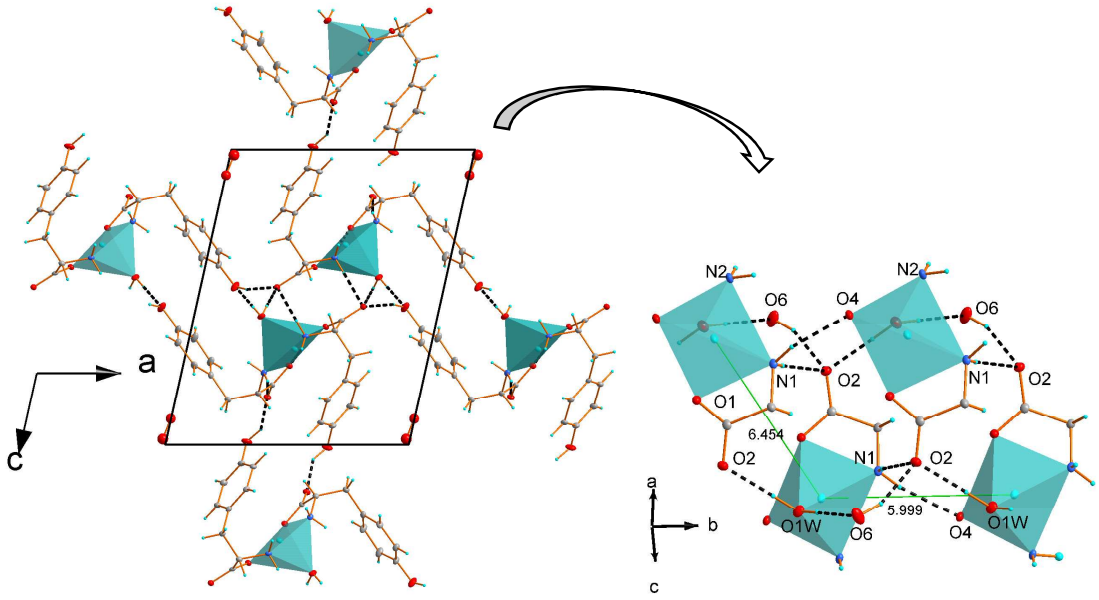

Fig. 2 (a) Crystal packing of **1** along *b* direction, disordered water accommodates empty voids in the crystal structure, (b) view perpendicular to *b* axis showing hydrogen bonds between neighboring centers, part of the ligands are not drawn for the picture clarity

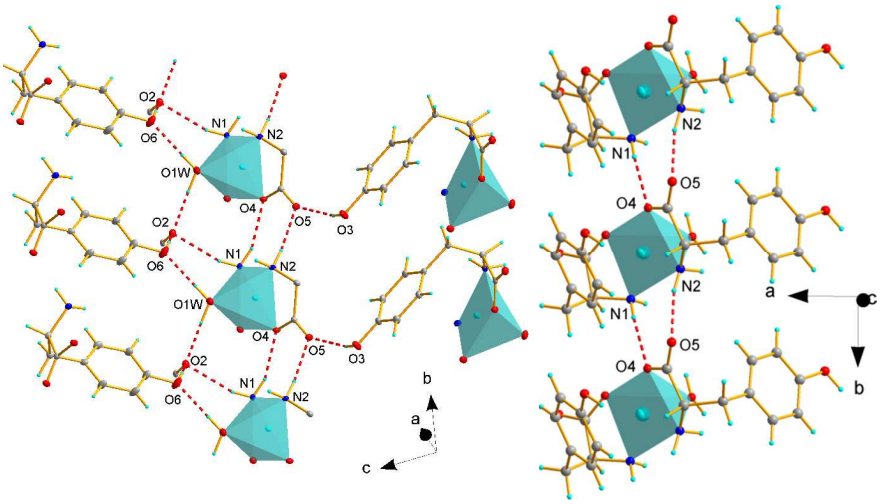

Fig. 3. Hydrogen bond interactions in $[Cu(L\text{-}Tyr)_2(H_2O)]\cdot H_2O$, part of the ligands are omitted for picture clarity.

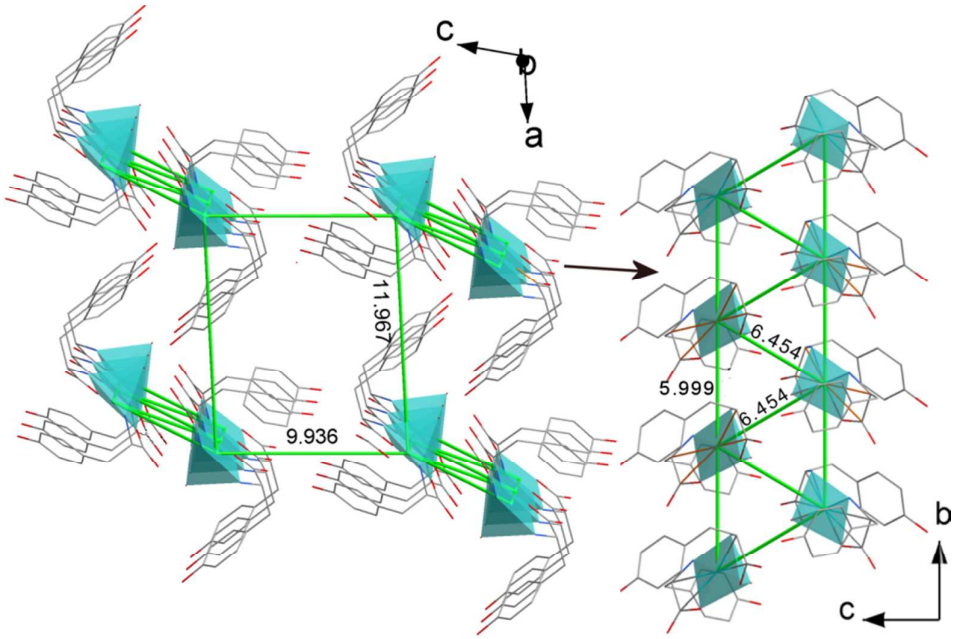

Fig. 4. The projection of the crystal structure of $[Cu(L\text{-}Tyr)_2(H_2O)]\cdot H_2O$ with marked distances between copper centers.

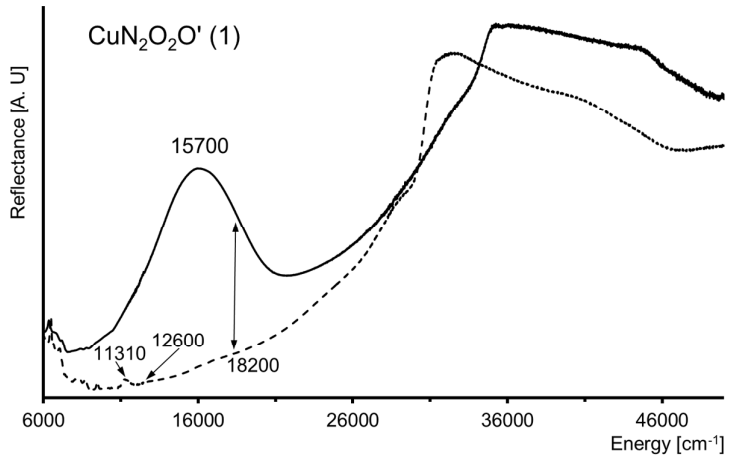

Fig. 5. Polycrystalline electronic reflectance spectrum of **1** (—) and pure L-tyrosine disodium salt (- - -) .

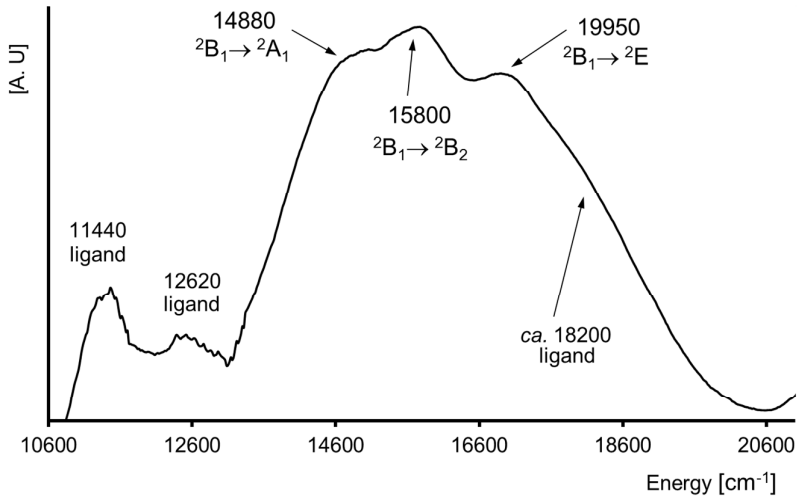

Fig. 6. The effect of filtration process of reflectance spectrum for **1** (visible region) (step = 20 cm^{-1}, α = 200 and N=30).

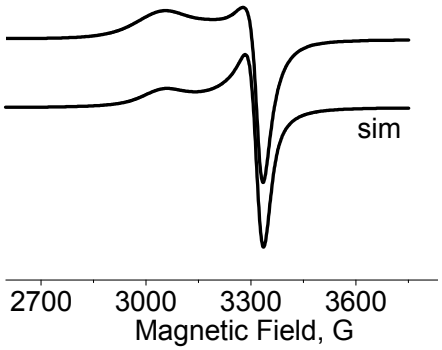

Fig. 7. X-band EPR spectra of powdered complex **1** at 77K simulated using the parameters given in the text .

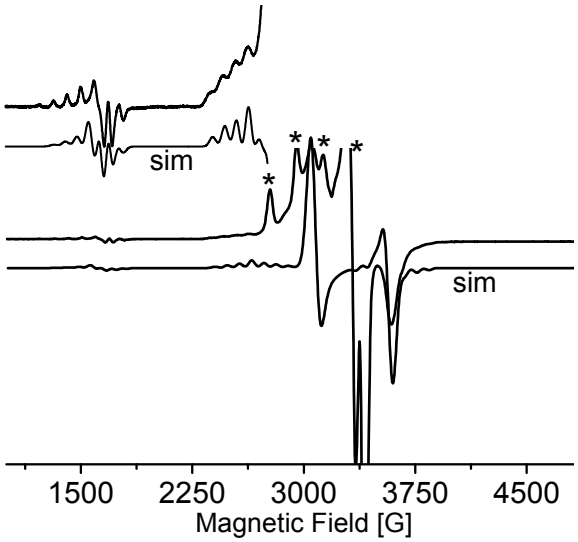

Fig. 8. EPR spectrum of the frozen DMSO solution of **1** together with the theoretical spectrum (sim), simulated using S=1 and the parameters given in the text. The stars indicate the signals due to monomeric S=1/2 complex from 1 (the first three lines are due to hyperfine interaction with one copper nuclei of parallel orientations). The above amplified fragment shows distinctly the hyperfine splitting due to two copper nuclei.

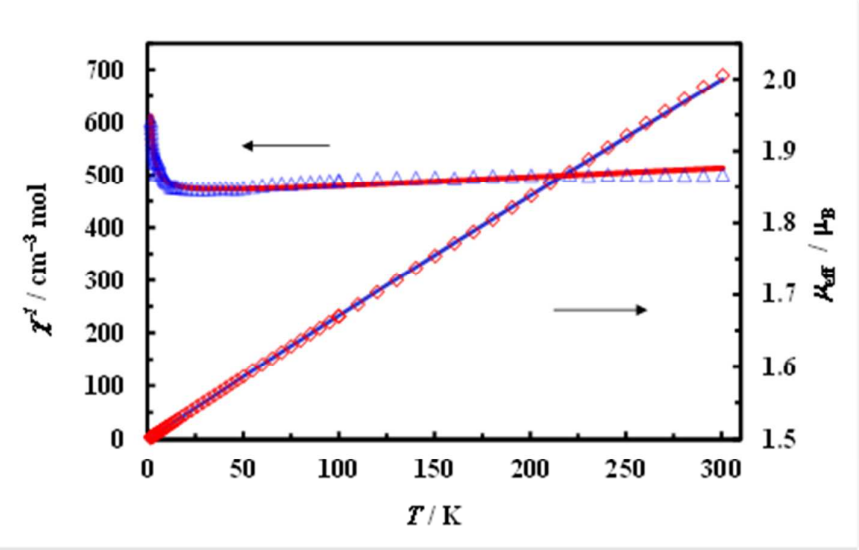

Fig. 9. Plots of reciprocal magnetic susceptibility, χ^{-1}, (◇) and effective magnetic moment, μ_{eff}, (Δ) versus temperature for [Cu(L-Tyr)$_2$(H$_2$O)]. The solid lines correspond to the best fit parameters (see the text).

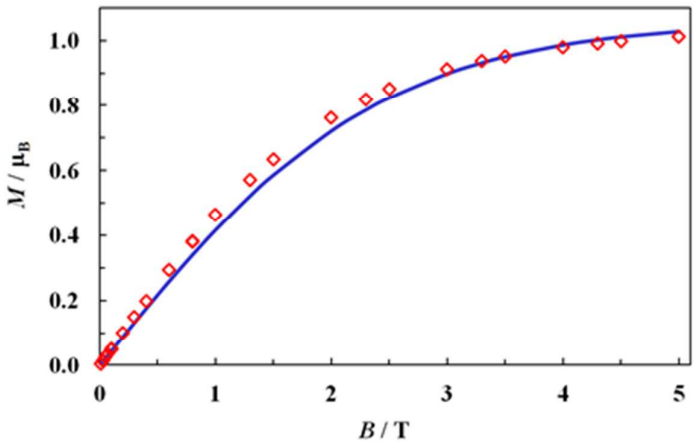

Fig. 10. Magnetization as a function of magnetic induction at 1.72 K. The line is the Brillouin function calculated for $S = ½$, $g = 2.1207$ (EPR average) and $N\alpha = 61 \cdot 10^{-6}$ emu/mol.

GRAPHICAL ABSTRACT

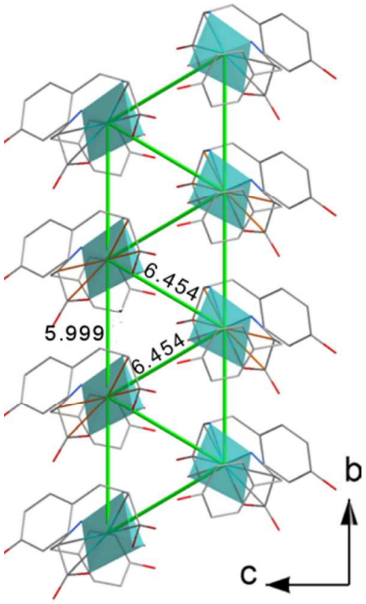

The L-tyrosinato copper(II) ions complex of formula [Cu(L-Tyr)$_2$(H$_2$O)]·H$_2$O (**1**) (where L-Tyr = L-tyrosine) was obtained as crystals and characterized by X-ray and spectroscopic (FT-IR, FT-Raman, NIR-vis-UV, and EPR) and magnetic methods. The N, O donors of chelating L-tyrosinato anions and O atom of coordinated water molecules form slightly distorted square pyramidal (SP) geometry around Cu(II) ions (τ = 0.113).